Ocean Dynamics (2006) 56: 295–307
DOI 10.1007/s10236-006-0064-3

Mark A. Powell · Robert J. Thieke · Ashish J. Mehta

Morphodynamic relationships for ebb and flood delta volumes at Florida's tidal entrances

Received: 27 January 2005 / Accepted: 5 January 2006 / Published online: 9 March 2006

Abstract Tidal entrances constitute an important boundary condition for the coastal ocean regime. Based on data from 67 sandy entrances in Florida, morphodynamic relationships between tidal prism, entrance throat area, and ebb and flood delta volumes are revisited. The main source of sand in these deltas is the littoral zone as opposed to the river. It is found that, as a rule of thumb, the volume of a mature ebb delta is equal to one fifth of the prism at the spring range of tide. Data for the coasts of Florida taken together indicate that the volume of mature flood delta varies with one third power of the prism. The Atlantic Coast flood delta volumes by themselves do not show any correlation with the prism, presumably because entrance depths have been altered by dredging. A case study of the closure of a land barrier breach at Matanzas Inlet illustrates the application of the derived morphodynamic relationships between prism, throat area, and ebb delta volume. These relationships are useful for prediction of changes in the throat area and the ebb delta volume when morphologic changes occur over time scales consistent with the reestablishment of equilibrium.

Keywords Littoral drift · Sand transport · Tidal hydraulics · Inlet morphology · Coastal sand resources · Sand budget

Responsible Editor: Alejandro Souza

M. A. Powell
Charles C. Isiminger Consulting Engineers,
649 US Highway 1, Suite 9,
North Palm Beach, FL 33408, USA

R. J. Thieke · A. J. Mehta (✉)
Department of Civil and Coastal Engineering,
University of Florida,
365 Weil Hall,
Gainesville, FL 32611, USA
e-mail: mehta@coastal.ufl.edu
Tel.: +1-352-3929537
Fax: +1-352-3923466

Introduction

Tidal entrances constitute an important dynamic boundary condition with respect to the coastal ocean regime due to their role as interfaces for exchange between seawater and embayed waters. Generalized morphodynamic relationships applicable to the entrances serve as useful tools for characterizing the physical state and the dynamic behavior of entrances. At sandy entrances, the three most important morphologic features are the channel, the ebb delta, and the flood delta. Because deltas exist due to water flow through the channel, the ebb and the flood delta volumes, V_e and V_f, respectively, depend on the channel throat cross-sectional area, A_c, i.e., the minimum flow area below mean tide level. As A_c is known to vary with the spring tidal prism, P, i.e., the water volume that enters the bay at (annual mean) spring tide, V_e and V_f, vary with P. The relationships $A_c(P)$, $V_e(P)$, and $V_f(P)$ play a key role in characterizing the link between the hydrodynamic and the morphologic regimes of the entrances and, in turn, the roles they play as sources or sinks of marine sediment. In this paper, we have reviewed the physical significance of these relationships based on data from sixty-seven sandy entrances in Florida (Fig. 1), where the maintenance of stable passages for navigation is vital to coastal commerce and recreational interests.

Area–prism relationship

Florida's Atlantic Coast with 28 entrances and the Gulf of Mexico Coast with 39 entrances are characterized by micro-tidal (<2 m) ranges R_o (Tables 1 and 2). The Atlantic tides are semi-diurnal, the panhandle coast tides from Pensacola Pass to East Pass at Carrabelle are mainly diurnal, and the lower Gulf Coast tides south of Anclote Pass are mixed. Representative values of the nearshore wave energy flux E_f in nominally 10-m water depth (Tables 1 and 2) indicate that the coastal wave energy in Florida is low to moderate compared to the US shorelines

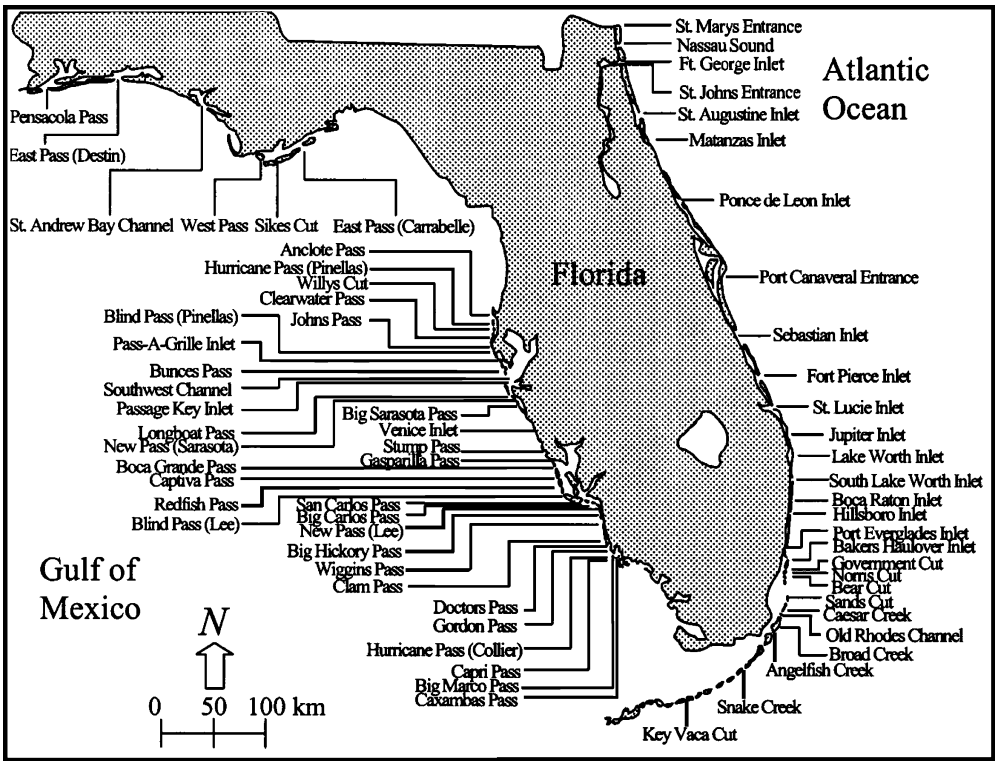

Fig. 1 Florida's tidal entrances

taken together, which also includes the high-wave-energy Pacific Coast (Walton and Adams 1976). Moreover, wave energy along the Gulf Coast is generally lower than along the Atlantic Coast. This difference is seemingly reflected in the median grain diameter of sand d_{50} of the ebb delta or the beach close to it (given in Tables 1 and 2). The d_{50} value is finer along the Gulf Coast (0.3 mm mean) compared to the Atlantic Coast (0.4 mm) presumably because smaller grains are winnowed out by the larger waves of the Atlantic. This difference is, however, too small to be of significance in differentiating the dynamics of the deltas at the two coasts and will not be invoked in the present analysis.

The well-known empirical relationship between the throat area and the spring tidal prism

$$A_c = aP^m \tag{1}$$

is applicable to entrance channels in live-bed sedimentary equilibrium. The coefficients a and m vary from entrance to entrance; however, O'Brien (1969) showed that for 28 US entrances, a=4.69×10^{-4} and m=0.85 as best-fit values are applicable to all entrances when P is measured in cubic meters (m^3) and A_c in square meters (m^2). For a sinusoidal variation of the flow discharge at the tidal frequency, P is related to mean discharge $\overline{Q}$ over flood or ebb flow duration by

$$P = \frac{T\overline{Q}}{2} \tag{2}$$

where T is the tidal period. Combining Eqs. 1 and 2 gives

$$A_c = a\left(\frac{T}{2}\right)^m \overline{Q}^m \tag{3}$$

For illustrative purposes, taking T=44,700 s for a semi-diurnal tide, we obtain

$$A = 2.30\overline{Q}^{0.85} \tag{4}$$

which is similar to

$$A = 1.51Q_r^{0.83} \tag{5}$$

where A is the river cross-sectional area and Q_r is the river discharge. Equation 5, known as the regime equation, was empirically derived for several non-tidal rivers in the US by Blench (1961). The analogy between river and tidal flows was pointed out by Mason (1973).

The transition between river-dominated flow and tide-dominated flow depends on the ratio of tide-mean discharge to river discharge $\overline{Q}/Q_r$. For river flow, $\overline{Q}/Q_r = 0$, and the influence of the river on tidal flow becomes minor when $\overline{Q}/Q_r \geq 20$. Although many small entrances in Florida are inundated by river outflows during spates, such events are relatively rare and, on an annual mean basis, the ratio $\overline{Q}/Q_r$ at all entrances is well above 20 (Bruun 1978). This, in turn, provides the justification for dealing with delta volumes in

Table 1 Atlantic Coast entrances

No.	Entrance	N lat. (°)	W long. (°)	Tidal range, R_o (m)	Wave energy flux, E_f[a] (N m/s m)	Grain size, d_{50} (mm)
1	St. Marys	30.72	81.43	1.9	8.09×10^3	0.3
2	Nassau Sound	30.50	81.42	1.8	9.62×10^3	0.4
3	Ft. George	30.42	81.42	1.8	8.20×10^3	0.2
4	St. Johns	30.40	80.40	1.8	8.20×10^3	0.2
5	St. Augustine	29.92	81.28	1.6	9.53×10^3	0.2
6	Matanzas	29.72	81.22	1.5	9.62×10^3	0.2
7	Ponce de Leon	29.08	80.92	1.3	1.56×10^4	0.2
8	Port Canaveral	28.40	80.58	1.2	1.36×10^4	0.4
9	Sebastian	27.87	80.43	1.1	1.34×10^4	0.3
10	Ft. Pierce	27.47	80.28	1.1	132×10^4	0.4
11	St. Lucie	27.17	80.17	1.0	9.59×10^3	0.4
12	Jupiter	26.95	80.08	1.0	8.35×10^3	0.3
13	Lake Worth	26.77	80.03	1.0	6.90×10^3	0.5
14	South Lake Worth	26.55	80.03	0.9	5.92×10^3	0.5
15	Boca Raton	26.33	80.06	0.9	4.79×10^3	0.5
16	Hillsboro	26.25	80.08	0.9	4.79×10^3	0.5
17	Port Everglades	25.93	80.12	0.9	4.79×10^3	0.5
18	Bakers Haulover	25.90	80.12	0.8	4.79×10^3	0.3
19	Government Cut	25.77	80.13	0.8	3.99×10^3	0.3
20	Norris Cut	25.75	80.15	0.8	3.99×10^3	0.3
21	Bear Cut	25.72	80.12	0.8	3.16×10^3	0.3
22	Sands Cut	25.50	80.18	0.8	3.99×10^3	0.7
23	Caesar Creek	25.38	80.23	0.8	3.99×10^3	0.7
24	Old Rhodes Channel	25.35	80.25	0.8	3.99×10^3	0.7
25	Broad Creek	25.35	80.25	0.8	3.99×10^3	0.7
26	Angelfish Creek	25.33	80.27	0.7	3.99×10^3	0.7
27	Snake Creek	24.95	80.58	0.7	3.99×10^3	0.7
28	Key Vaca Cut	24.72	81.03	0.6	1.93×10^3	0.7

[a] $E_f = \rho g H^2 L/8T_w$, where ρ=seawater density, g=acceleration due to gravity, H=(annual mean) significant wave height, T_w=(annual mean) wave modal period, and L=wave length

terms of their dependence on the tidal prism, without invoking the influence of river discharge.

The basis of Eq. 4 can be examined by considering sand transport in rivers. At a given flow velocity u ($=Q_r/A$), when the bottom shear stress τ is greater than the critical shear stress for erosion τ_c under live-bed equilibrium, the number of sand grains eroding from the bed (by saltation) per unit bed area per unit time equals the number depositing from suspension per unit bed area per unit time. The resulting sand unit load q_s, i.e., sand volume per unit time per unit channel width, is dependent on τ. A well-known expression for this dependence is the Einstein-Brown approximation of the Einstein's bedload equation for sand transport (see, e.g., Graf 1971)

$$\varphi = 40\psi^3 \tag{6}$$

in which the bedload function ϕ and the Shields' parameter ψ, are, respectively,

$$\varphi = \frac{q_s}{w_s d} \tag{7}$$

$$\psi = \frac{\tau}{\gamma(s-1)d} = \frac{\rho u_*^2}{\gamma(s-1)d} \tag{8}$$

with

$$u_* = u\left(\frac{f}{8}\right)^{1/2} \tag{9}$$

Table 2 Gulf Coast entrances

No.	Entrance	N lat. (°)	W long. (°)	Tidal range, R_o (m)	Wave energy flux, E (N m/s m)	Grain size, d_{50} (mm)
29	Caxambas Pass	25.90	81.72	0.9	1.96×10^3	0.3
30	Big Marco Pass	25.97	81.73	0.9	1.98×10^3	0.3
31	Capri Pass	25.98	81.75	0.9	1.98×10^3	0.3
32	Hurricane Pass (Collier)	26.00	81.75	0.9	1.98×10^3	0.3
33	Gordon Pass	26.08	81.80	0.9	1.98×10^3	0.2
34	Doctors Pass	26.17	81.68	0.9	1.98×10^3	0.2
35	Clam Pass	26.22	81.82	0.9	1.98×10^3	0.2
36	Wiggins Pass	26.30	81.83	0.9	1.95×10^3	0.2
37	Big Hickory Pass	26.37	81.87	0.8	1.95×10^3	0.2
38	New Pass	26.38	81.87	0.8	1.95×10^3	0.2
39	Big Carlos Pass	26.40	81.88	0.8	1.95×10^3	0.2
40	San Carlos Pass	26.47	81.97	0.8	1.94×10^3	0.4
41	Blind Pass (Lee)	26.47	82.18	0.8	1.94×10^3	0.4
42	Redfish Pass	26.55	82.20	0.7	1.94×10^3	0.4
43	Captiva Pass	26.60	82.23	0.7	1.94×10^3	0.5
44	Boca Grande Pass	26.72	82.27	0.7	1.94×10^3	0.4
45	Gasparilla Pass	26.82	82.28	0.7	1.42×10^3	0.3
46	Stump Pass	26.90	82.35	0.7	1.96×10^3	0.5
47	Venice Inlet	27.12	82.47	0.7	1.94×10^3	0.8
48	Big Sarasota Pass	27.28	82.57	0.7	2.53×10^3	0.1
49	New Pass	27.32	82.58	0.8	2.53×10^3	0.2
50	Longboat Pass	27.43	82.68	0.7	1.94×10^3	0.2
51	Passage Key Channel	27.55	82.75	0.7	2.53×10^3	0.3
52	Southwest Channel	27.55	82.77	0.7	2.53×10^3	0.3
53	Egmont Channel	27.62	82.77	0.7	2.54×10^3	0.3
54	Bunces Pass	27.65	82.73	0.7	1.94×10^3	0.3
55	Pass-A-Grille Channel	27.68	82.73	0.7	1.94×10^3	0.3
56	Blind Pass (Pinellas)	27.73	82.75	0.7	1.94×10^3	0.4
57	Johns Pass	27.78	82.78	0.8	2.53×10^3	0.4
58	Clearwater Pass	27.97	82.83	0.8	2.56×10^3	0.2
59	Willys Cut	28.05	82.82	0.9	2.56×10^3	0.2
60	Hurricane Pass (Pinellas)	28.05	82.83	0.9	2.56×10^3	0.2
61	Anclote Pass	28.18	82.80	0.9	2.00×10^3	0.2
62	East Pass (Carrabelle)	29.77	84.68	0.6	1.95×10^3	0.3
63	Sikes Cut	29.62	84.97	0.5	2.54×10^3	0.3
64	West Pass	29.63	85.10	0.5	2.54×10^3	0.3
65	St. Andrew Bay Channel	30.10	85.72	0.4	2.52×10^3	0.3
66	East Pass (Destin)	30.40	86.52	0.4	2.52×10^3	0.3
67	Pensacola Pass	30.34	87.32	0.4	5.01×10^3	0.3

In the above equations, w_s is the settling velocity of a grain of diameter d, γ is the unit weight of water, $s=\gamma_s/\gamma$ is the specific weight of sand grains, γ_s is their unit weight, $u_* = \sqrt{g\tau/\gamma}$ is the flow friction velocity, and f is the Darcy–Weisbach friction factor.

In sufficiently energetic rivers and tidal entrances, suspended load transport usually dominates over bedload. Christensen and Chiu (1973) argued that, as both modes of transport involve sediment exchange between the bed and the suspension, q_s can be considered to represent the total load, i.e., the sum of suspended load and bedload. They supported this assumption by showing the application of an Einstein-type bedload equation to data on total load of sand measured in flumes. As this approach obviates the need to differentiate between the two types of loads, we will consider Eq. 6 to represent the total load. From Eqs. 6 through 9, we obtain

$$\frac{q_s}{w_s} = \frac{0.078 f^3}{g^3 (s-1)^3 d^2} u^6 \tag{10}$$

where q_s now denotes total unit load. This equation can be restated as

$$q_s = \frac{0.078 f^3 w_s}{g^3 (s-1)^3 d^2} \left(\frac{\overline{Q}}{A_c}\right)^6 = K_1 \left(\frac{\overline{Q}}{A_c}\right)^6 \quad (11)$$

in which $K_1 = 0.078 f^3 w_s \Big/ g^3 (s-1)^3 d^2$. For a given entrance channel, we may treat K_1 as a constant. For such a channel in live-bed equilibrium, the ratio $\overline{Q}/A_c$ is obtained from Eq. 3 as

$$\frac{\overline{Q}}{A_c} = K_2 \overline{Q}^{1-m} \quad (12)$$

where $K_2 = (2/T)^2 \Big/ a$. Hence, combining Eqs. 11 and 12, we get

$$q_{so} = K_1 K_2^6 \overline{Q}^{6(1-m)} \quad (13)$$

where q_s=q_{so} is now the unit load of sand under live-bed equilibrium. An expression obtained by Kraus (1998) using a different formula for sediment transport can be interpreted in the same way as Eq. 13. It is a restatement of Eq. 1, and as m=0.85, for a given entrance, q_{so} is proportional to $\overline{Q}^{0.09}$. A set of data on 162 entrances along the US shorelines indicates that m ranges between 0.84 and 1.10 (Jarrett 1976). Thus, the exponent of $\overline{Q}$ ranges from 0.96 to −0.60, implying a reversal in the

Table 3 Atlantic Coast entrance deltas

No.	Entrance	Mean depth, h_c (m)	Flow area, A_c (m^2)	Tidal prism, P (m^3)	Ebb delta volume, V_e (m^3)	Flood delta volume, V (m^3)
1	St. Marys	12.7	1.2×10^4	3.3×10^8	2.5×10^8	1.55×10^6
2	Nassau Sound	4.3	6.8×10^3	6.8×10^7	4.1×10^7	NA
3	Ft. George[a]	3.8	8.7×10^2	1.6×10^7	1.3×10^8	9.54×10^5
4	St. Johns[a]	8.4	4.2×10^3	1.2×10^8		NA
5	St. Augustine	10.8	4.6×10^3	2.5×10^7	4.3×10^7	1.34×10^6
6	Matanzas	2.8	9.1×10^2	1.4×10^7	4.8×10^6	1.27×10^5
7	Ponce de Leon	3.4	1.5×10^3	1.7×10^7	1.7×10^7	2.86×10^6
8	Port Canaveral	15.0	3.0×10^3	2.6×10^6	NS	NA
9	Sebastian	2.3	3.6×10^2	8.5×10^6	1.2×10^6	1.19×10^6
10	Ft. Pierce	6.3	1.7×10^3	4.4×10^7	2.3×10^7	NA
11	St. Lucie	3.2	1.5×10^3	1.8×10^7	3.8×10^6	2.85×10^6
12	Jupiter	2.3	2.7×10^2	7.6×10^6	5.0×10^5	7.33×10^5
13	Lake Worth	5.7	1.4×10^3	2.4×10^7	2.9×10^6	NA
14	South Lake Worth	3.3	1.0×10^2	3.0×10^6	3.9×10^6	3.55×10^6
15	Boca Raton	3.6	1.8×10^2	4.9×10^6	8.0×10^5	9.36×10^6
16	Hillsboro	4.2	3.2×10^2	8.1×10^6	NS	NA
17	Port Everglades	9.8	2.9×10^3	1.9×10^7	NS	NA
18	Bakers Haulover	4.3	5.2×10^2	1.8×10^7	2.1×10^6	4.39×10^5
19	Government Cut	4.7	1.4×10^3	2.7×10^7	NS	NA
20	Norris Cut	2.3	1.5×10^3	3.1×10^7	NS	5.47×10^5
21	Bear Cut	5.2	6.0×10^3	4.6×10^7	NS	4.97×10^6
22	Sands Cut	2.5	2.1×10^2	2.2×10^6	NS	1.66×10^6
23	Caesar Creek	3.1	1.6×10^3	2.5×10^7	1.5×10^7	1.40×10^6
24	Old Rhodes Channel[a]	2.9	2.9×10^2	2.0×10^5	4.4×10^5	3.97×10^6
25	Broad Creek[a]	2.1	1.4×10^3	2.1×10^7		2.60×10^6
26	Angelfish Creek[a]	3.7	8.5×10^2	1.1×10^7		1.22×10^6
27	Snake Creek	2.1	3.8×10^2	1.6×10^7	NS	1.51×10^6
28	Key Vaca Cut	2.5	4.5×10^2	5.1×10^6	NS	1.65×10^6

NS No significant ebb delta volume due to deep entrance channel or other features, *NA* data not available
[a]Ebb delta volumes combined

Table 4 Gulf Coast entrance deltas

No.	Entrance	Mean depth, h_c (m)	Flow area, A_c (m^2)	Tidal prism, P (m^3)	Ebb delta volume, V_e (m^3)	Flood delta volume, V_f (m^3)
29	Caxambas Pass	1.1	6.8×10^{2}	6.3×10^{6}	2.86×10^{6}	6.58×10^{6}
30	Big Marco Pass	5.0	1.5×10^{3}	4.4×10^{7}	1.06×10^{7}	4.26×10^{6}
31	Capri Pass	3.7	2.6×10^{3}	4.1×10^{7}	1.57×10^{6}	1.57×10^{6}
32	Hurricane Pass (Collier)	2.7	5.9×10^{2}	5.2×10^{6}	1.64×10^{6}	1.61×10^{6}
33	Gordon Pass	3.1	9.4×10^{2}	1.2×10^{7}	7.79×10^{5}	9.10×10^{5}
34	Doctors Pass	2.3	1.1×10^{2}	9.3×10^{5}	2.19×10^{5}	NA
35	Clam Pass	0.4	2.6×10^{1}	3.3×10^{5}	1.49×10^{5}	3.06×10^{4}
36	Wiggins Pass	1.8	1.3×10^{2}	1.4×10^{6}	5.96×10^{5}	4.58×10^{5}
37	Big Hickory Pass	1.4	5.9×10^{1}	1.2×10^{6}	4.74×10^{5}	6.67×10^{5}
38	New Pass	3.6	4.1×10^{2}	7.6×10^{6}	8.87×10^{5}	8.23×10^{5}
39	Big Carlos Pass	1.8	1.1×10^{3}	2.0×10^{7}	4.09×10^{6}	5.50×10^{6}
40	San Carlos Pass	4.6	2.4×10^{4}	5.9×10^{8}	3.55×10^{7}	3.55×10^{7}
41	Blind Pass (Lee)	2.1	6.4×10^{1}	1.2×10^{6}	Minor	4.97×10^{4}
42	Redfish Pass	8.0	1.6×10^{3}	1.4×10^{7}	3.31×10^{6}	2.17×10^{6}
43	Captiva Pass	3.6	2.2×10^{3}	5.4×10^{7}	7.89×10^{6}	1.13×10^{7}
44	Boca Grande Pass	7.6	9.3×10^{3}	3.6×10^{8}	7.41×10^{7}	9.77×10^{6}
45	Gasparilla Pass	0.6	4.1×10^{2}	1.3×10^{7}	6.29×10^{6}	1.86×10^{7}
46	Stump Pass	1.4	2.4×10^{2}	4.2×10^{6}	5.73×10^{5}	2.21×10^{6}
47	Venice Inlet	3.2	2.5×10^{2}	3.0×10^{6}	1.18×10^{6}	2.16×10^{6}
48	Big Sarasota Pass	2.8	1.5×10^{3}	3.5×10^{7}	3.80×10^{6}	1.18×10^{7}
49	New Pass	3.4	7.4×10^{2}	1.8×10^{7}	4.21×10^{6}	1.20×10^{6}
50	Longboat Pass	3.2	9.0×10^{2}	1.6×10^{7}	5.05×10^{6}	3.61×10^{6}
51	Passage Key Channel	4.0	4.8×10^{3}	9.2×10^{7}	3.01×10^{7}	6.23×10^{6}
52	Southwest Channel	5.4	1.1×10^{4}	2.4×10^{8}	2.22×10^{7}	3.14×10^{6}
53	Egmont Channel	7.1	1.8×10^{4}	6.2×10^{8}	1.68×10^{7}	9.50×10^{6}
54	Bunces Pass	3.7	1.4×10^{3}	1.2×10^{7}	9.18×10^{6}	3.42×10^{6}
55	Pass-A-Grille Channel	4.0	3.1×10^{3}	2.9×10^{7}	4.32×10^{6}	3.69×10^{6}
56	Blind Pass (Pinellas)	1.5	2.3×10^{2}	4.6×10^{6}	8.79×10^{5}	1.61×10^{6}
57	Johns Pass	6.1	1.3×10^{3}	1.9×10^{7}	1.47×10^{6}	2.83×10^{6}
58	Clearwater Pass	3.4	1.5×10^{3}	2.1×10^{7}	1.53×10^{6}	1.54×10^{6}
59	Willys Cut[a]	1.4	5.7×10^{2}	3.9×10^{6}	1.76×10^{5}	NA
60	Hurricane Pass (Pinellas)[a]	3.0	6.5×10^{2}	1.0×10^{7}		9.52×10^{5}
61	Anclote Pass	3.3	1.7×10^{3}	1.8×10^{7}	4.74×10^{6}	1.96×10^{6}
62	East Pass (Carrabelle)	4.6	1.3×10^{4}	3.3×10^{8}	1.22×10^{7}	9.14×10^{6}
63	Sikes Cut	3.0	2.0×10^{2}	2.2×10^{6}	1.68×10^{5}	8.35×10^{6}
64	West Pass	6.2	3.9×10^{3}	7.6×10^{7}	1.41×10^{7}	1.43×10^{7}
65	St. Andrew Bay Channel	3.7	4.6×10^{3}	4.2×10^{7}	2.55×10^{5}	3.81×10^{6}
66	East Pass (Destin)	2.8	1.6×10^{3}	4.4×10^{7}	1.66×10^{7}	5.23×10^{6}
67	Pensacola Pass	12.8	1.0×10^{4}	2.7×10^{8}	1.13×10^{6}	3.50×10^{6}

NA No data
[a]Ebb delta volumes combined

dependence of q_{so} on $\overline{Q}$ from almost linear to approximately $1/\overline{Q}$.

For 8 out of 28 entrances without jetties, O'Brien (1969) showed that Eq. 1 could be applied with $a = 2\times10_{-5}$ and m=1, supporting an earlier observation of LeConte (1905) inferred from data on five California entrances. According to LeConte, "Nature requires 33 sq. ft of mean-tide section for each and every million cubic feet of tidal waters passing in and out at spring tides". Given the area in square meters and the prism in cubic meters, this amounts to $a = 1.08\times10_{-4}$ and m=1. For sheltered harbors, LeConte recommended $a = 1.41\times10^{-4}$ and m=1. The value of m equal to unity in these instances means that q_{so} is independent of $\overline{Q}$ and $K_2 = T/2a$. Area–prism data in Tables 3 and 4, compiled from the literature by Powell (2003) and plotted in Fig. 2, corroborate this observation. The best-fit values of the coefficients of Eq. 1 are $a = 7.25\times10^{-5}$ and m=0.97 (which is close to 1) with a correlation coefficient r^2=0.67. Port Canaveral Entrance is an artificial channel without a direct connection to the interior waters, and its throat area,

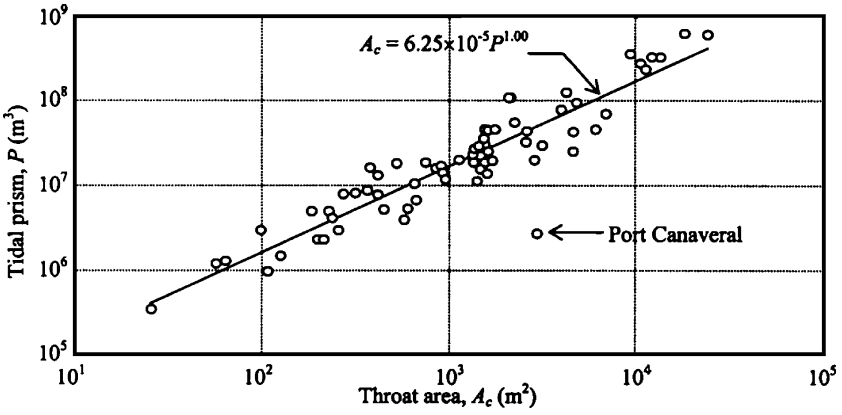

Fig. 2 Area–prism data for Florida entrances. The best-fit line excludes Port Canaveral Entrance, an artificial harbor without a bay

maintained by dredging, is much larger than the equilibrium value corresponding to the entrance's tidal prism. Excluding this entrance yields $a = 6.25\times10^{-5}$ and m=1 with r^2=0.91.

Equation 13 implies that, at an entrance which conforms to Eq. 1, the sand unit load is q_{so}. Thus, for entrances for which K_1, K_2, $\overline{Q}$, and m are known, q_{so} can be calculated. Consider this example: T=44,712 s (semi-diurnal tide), $a = 6.25\times10^{-5}$, m=1, w_s=0.04 m s^{-1} (corresponding to d=3×10^{-3} m), f=0.028 (from Bruun 1978), and s=2.65 (quartz sand). With these values, we obtain K_1=1.79×10^{-4} and K_2=0.716. Hence, from Eq. 13, q_{so}=2.41×10^{-5} m^2 s^{-1}. So, for an entrance that is, say, 100-m wide, taking 2,650 kg m^{-3} as the granular density of sand, this value of q_{so} amounts to the transport of 143 t of sand over one half tidal period (ebb or flood) or 2.05×10^5 t year^{-1}.

The sand entering Florida's entrances is predominantly littoral, i.e., from the open coasts as opposed to the interior waters. The annual rate of sand transport into six entrances based on dredging records is given in Table 5 (Jones and Mehta 1980). This *net* rate should be comparable to the *gross* rate during flood tidal flow provided that all or, at least, the majority of sand deposits in the channel. Dredging records and growth rates of flood deltas indicate at least an order of magnitude higher rate of sand deposition in the channel compared to the ebb delta. In other words, the majority of sand which enters during flood tide deposits in the channel (Bruun 1978). Therefore, we may take the sand transport rate derived from deposition in the channel to be an approximate measure of q_{so}.

For the net unit load q_{so}, Table 5 indicates a range of 8.01×10^{-6} to 4.23×10^{-5} m^2 s^{-1}, and 1.1×10^5 to 2.95×10^5 t year^{-1} for the net load, i.e., unit load multiplied by channel width. The net load is surprisingly uniform, and neither it nor the unit load correlates with the wave energy flux, E_f, the main transporting agent for littoral drift. This suggests that the morphology of the channel and the deltas plays an important role in governing sand transport in the channel.

Ebb delta volume vs prism

The volume V_e and the crescentic shape of the ebb delta (Fig. 3) are determined by the tidal current and the sea waves. At Jupiter Inlet on the Atlantic Coast (Fig. 4), the ebb delta grew rapidly in the initial years after this entrance was fully opened by capital dredging and stabilized by jetties in 1947. The mean growth rate was 38,000 m^3 per year during the first decade. After about two decades, the delta attained a quasi-equilibrium state or maturity under the counterbalancing roles of tide in depositing sand and waves in removing it. Year-to-year changes in this balance caused the volume to oscillate about a long-term mean of about 5×10^5 m^3, notionally bounded by a high 7.8×10^5 m^3 and a low 2.2×10^5 m^3. Dombrowski and Mehta (1996) characterized these bounds by a dimensionless number representing the ratio of wave energy flux to tidal energy flux. As the latter can be assumed to remain invariant on the annual mean basis, the wave energy determines the bounds; the upper bound corresponds to a low wave height and the lower bound to a larger wave height. Devine and Mehta (1999) showed that the delta lobe face (Fig. 3a) recedes by erosion under high waves and recovers when wave action subsides, in a manner similar to the submerged portion of a sandy beach.

Table 5 Annual sand loads at six entrances from dredging records

Entrance	Width, w_c (m)	Wave energy flux, E_f (N m s^{-1} m^{-1})	Net sand unit load (m^2 s^{-1})	Net sand load (t year^{-1})
Ponce de Leon	440	1.6×10^4	8.01×10^{-6}	2.95×10^5
Sebastian	160	1.3×10^4	8.26×10^{-6}	1.10×10^5
Jupiter	120	8.4×10^3	8.24×10^{-6}	1.17×10^5
Boca Raton	50	4.8×10^3	4.23×10^{-5}	1.77×10^5
Hillsboro	75	4.8×10^3	2.04×10^{-5}	1.28×10^5
East Pass (Destin)	340	2.5×10^3	5.05×10^{-6}	1.44×10^5

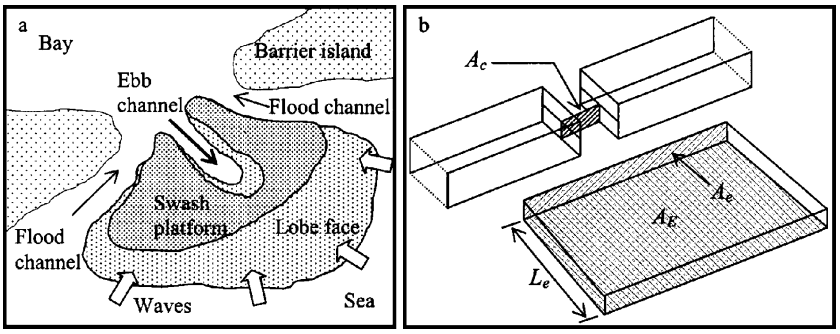

Fig. 3 **a** Ebb delta features **b** Idealized geometry

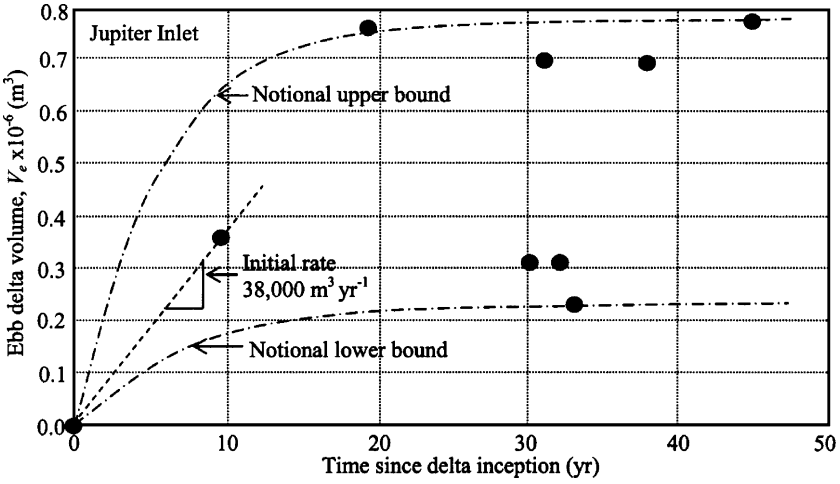

Fig. 4 Growth of ebb delta at Jupiter Inlet since 1947

The ebb delta volumes in Tables 3 and 4 were calculated by applying the graphical method of Dean and Walton (1975) to isobaths at the delta along with those at the nearby shorelines unaffected by the delta. The volumes represent deltas that are, at least, a decade old and, in many cases, older than five decades. At such mature deltas, the following argument allows us to ascertain the dependence of the delta volume on the tidal prism.

Figure 3b is a rendition of the ebb delta idealized as a box of lateral area A_e, planform area A_E and length L_e. The delta volume is

$$V_e = A_e L_e \tag{14}$$

As A_e can be expected to vary with the size of the entrance, we will assume that A_e is geometrically related to the throat area A_c according to

$$A_e = c_0 A_c^{n_0} \tag{15}$$

where c_0 and n_0 are entrance-specific constants. Values of c_0 are generally not available; however, De Vriend et al. (2002) selected n_0=1. Substituting Eq. 1 into Eq. 15 gives

$$A_e = c_0 a^m P^{n_0 m} \tag{16}$$

Based on the data of Gibeaut and Davis (1993) from 21 entrances on the Gulf Coast between Caxambas Pass and Hurricane Pass (Pinellas), Dombrowski and Mehta (1996) obtained the following approximate dependence of A_E on the prism P

$$A_E = c_1 P^{n_1} \tag{17}$$

where $c_1 = 2.54/R_o^{n_1}$ and n_1=0.81 with r^2=0.65. In Table 2, the tidal range R_o along the segment of the Gulf Coast where these entrances occur is seen to be reasonably uniform, varying narrowly between 0.7 and 0.9 m. We may accordingly and conveniently take c_1 to be independent of R_o and further assume that Eq. 17 is applicable to all entrances.

Table 6 Coefficients for ebb delta volume vs tidal prism relation

Entrances	Coefficient, c_e	Coefficient, n_e	Correlation coefficient, r^2
All	4.05×10^{0}	0.82	0.59
Atlantic Coast	3.80×10^{-3}	1.26	0.57
Gulf Coast	1.41×10^{1}	0.73	0.70
Gulf Coast less Willys Cut/Hurricane Pass	1.71×10^{1}	0.72	0.75

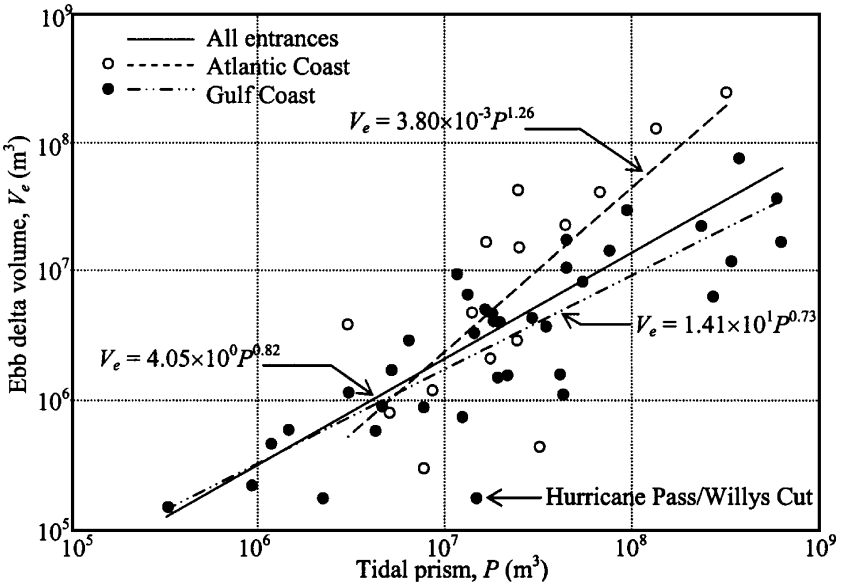

Fig. 5 Ebb delta volume vs tidal prism

From Fig. 3b, by way of geometric scaling $L_e \sim A_E^{1/2}$ or in general

$$L_e = c_2 A_E^{n_2} \tag{18}$$

an inference supported by the analysis of Vincent and Corson (1981) on 67 entrances along the US shorelines. They reported c_2=0.3 and n_2=0.58 (which is reasonably close to 0.50). Combining Eqs. 17 and 18, we obtain

$$L_e = c_2 c_1^{n_2} P^{n_1 n_2} \tag{19}$$

where c_2 is another constant. Finally, combining Eqs. 14, 16, and 19 yields

$$V_e = c_0 c_1^{n_2} c_2 a^m P^{n_0 m + n_1 n_2} = c_e \rho^{n_e} \tag{20}$$

where $c_e = c_0 c_1^{n_2} c_2 a^m$ and $n_e = n_0 m + n_1 n_2$. Selecting n_0=1, m=0.97, n_1=0.81, and n_2=0.58, we obtain n_e=1.44.

The best-fit values of c_e and n_e for the Florida entrances are given in Table 6. In Fig. 5, three lines are shown, one including all 57 entrances for which ebb deltas are reported, one line for the 19 Atlantic Coast entrances, and the last line for the 38 Gulf Coast entrances. Gulf data are also given without including Willys Cut and Hurricane Pass (Pinellas). These adjacent entrances effectively contain a single ebb delta whose value is uncertain because the bathymetry used was of poor quality and uncertain date.

The value n_e=1.26 for the Atlantic Coast is smaller than 1.44 by 13% but only 2% greater than n_e=1.23 obtained consistently by Walton and Adams (1976) for all three US shorelines. These investigators also showed that c_e decreases with increasing wave energy, indicating that, for a given prism, the ebb delta volume decreases with

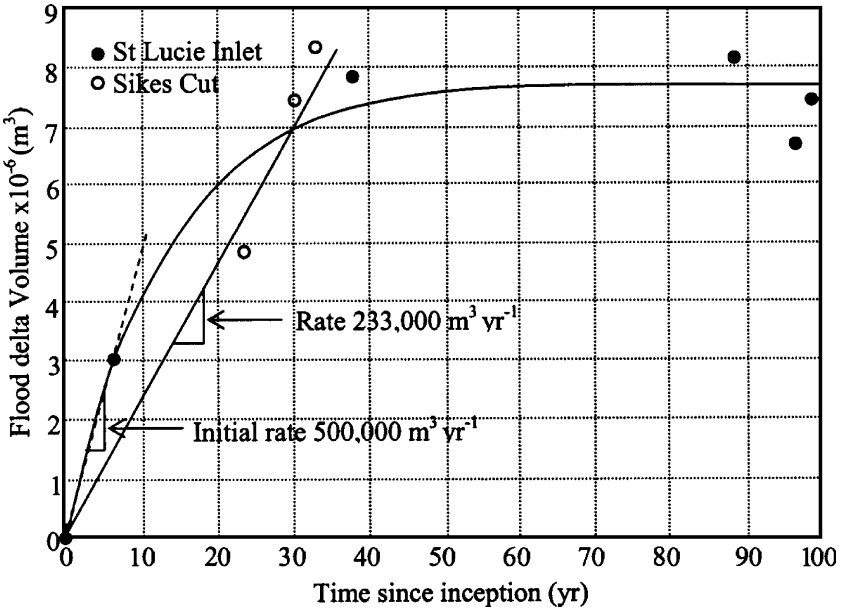

Fig. 6 Growth of flood deltas at Sikes Cut (since 1954) and St. Lucie Inlet (since 1892)

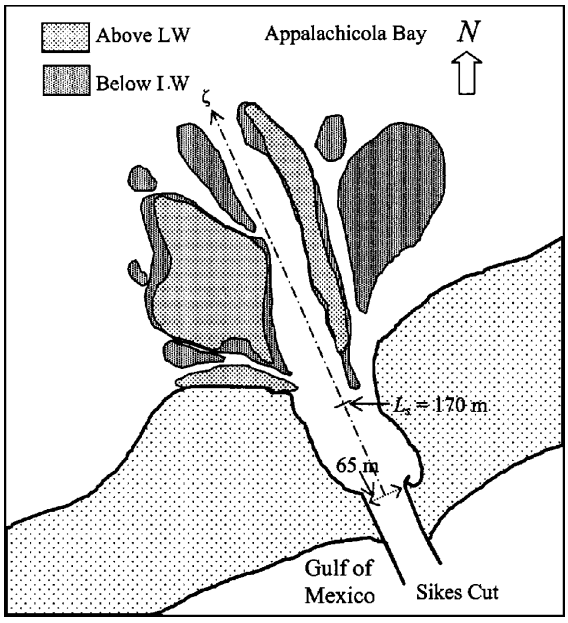

Fig. 7 Flood delta at Sikes Cut

increasing wave energy. This is so because, with increasing wave energy, the sand-winnowing role of waves increases relative to the sand-depositing role of ebb flow. Unfortunately, as the wave energy flux E_f along the coasts of Florida varies over a narrow range compared with the US shorelines as a whole (Walton and Adams 1976), any effect of E_f on delta volume cannot be discerned from the "noisy" V_e values.

Dombrowski and Mehta (1996) concluded that, due to uncertainties associated with bathymetric data and subjectivity in delineating the ebb delta geometry, the error in estimating V_e according to the Dean and Walton (1975) method can be as much as ±10% and possibly higher in cases involving complicated shoreline and entrance configurations. At 16 entrances between St. Marys and Hillsboro on the Atlantic Coast, the mean depth is generally more than twice in dredged entrances (7 m) compared to the ones that remain natural or undredged (3.1 m). Thus, channel dredging has influenced delta volume, possibly quite significantly in some cases.

From Table 6, we observe that a plausible value of n_e for the Florida coast as a whole is equal to 1. With this value, we obtain c_e=0.2. In other words, as a rule of thumb, the mean ebb delta volume is one fifth of the spring tidal prism.

Flood delta volume vs prism

Flood deltas are shaped by tidal flow without the counteracting influence of sea waves, even as these waves "push" littoral sand into the entrance. At a new entrance, the delta volume increases rapidly in the initial years. At Sikes Cut on the Gulf Coast, the growth rate of the delta in Appalachicola Bay during the first three decades, since this entrance was opened in 1954, was seemingly constant at 233,000 m^3 $year^{-1}$ (Fig. 6). In contrast, at St. Lucie Inlet on the Atlantic Coast, where the bay area is restricted by the width of the embayment, the growth rate (500,000 m^3 $year^{-1}$, Fig. 6) decreased after the first decade from the time the entrance was newly dredged in 1892. About four decades later, the volume stabilized, with practically no further change within a ±15% error band characteristic of generally well-defined flood delta estimates. In general, where an identifiable flood delta volume is limited by bay size, sand continues to arrive from the sea and to deposit in the upstream reaches (Carr de Betts and Mehta 2001). The excess sand is often dredged to maintain navigable depths, e.g., in the Intracoastal Waterway between the barrier island and the mainland.

Regardless of bay size, the thickness h_f of mature deltas appears to vary over a narrow range. Based on the histogram of the thicknesses of 61 flood deltas in Florida, Carr de Betts and Mehta (2001) observed that the majority of values ranged between 0.7 and 1.1 m, with a mean very close to 1 m. Most of these deltas occurred in conditions defined by narrow ranges of characteristic physical parameters: micro-tidal range, water depth of 2 to 5 m, strength of flood current from 0.8 to 1.1 m s^{-1}, and grain size from 0.2 to 0.7 mm. One may surmise that the constant delta thickness of 1 m is a manifestation of live-bed sedimentary equilibrium locally over the flood delta. At a new entrance, once the thickness of the deposit reaches 1 m, subsequent incoming sand is pushed further inward, causing the delta to expand and fan out.

In analogy with Eq. 14, the flood delta volume is

$$V_f = A_f L_f = h_f w_f L_f \tag{21}$$

where A_f is the cross-sectional area, L_f the length, and w_f the width of the delta "box". The simplest idealization of delta growth can be parameterized in terms of a constant h_f, e.g., 1 m, a constant w_f governed by the flood-flow jet and L_f increasing along the longitudinal distance ζ at a decreasing rate until the delta acquires a mature, quasi-steady volume.

Table 7 Coefficients for flood delta volume vs tidal prism relation

Entrances	Coefficient, c_f	Coefficient, n_f	Correlation coefficient, r^2
All	8.41×10^3	0.34	0.23
Atlantic Coast	–	–	–
Gulf Coast	1.01×10^3	0.48	0.38
Gulf Coast less Clam Pass	6.95×10^3	0.37	0.47

– No correlation found

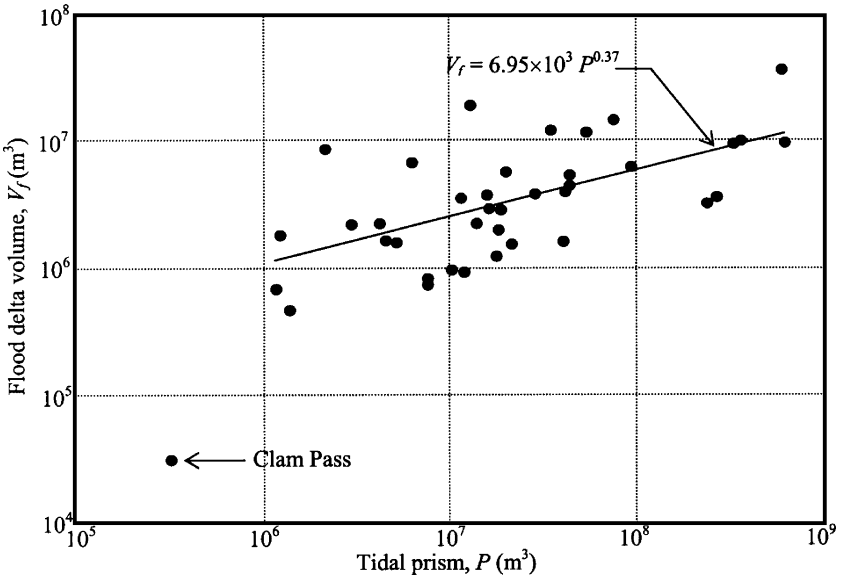

Fig. 8 Flood delta volume vs tidal prism; Florida's Gulf Coast entrances

The width w_f may be estimated as follows. A simple model for the increase in flow jet width w with ζ is given by

$$\frac{w(\zeta)}{w_c} = e^{\frac{f}{16h}\zeta} \tag{22}$$

where w_c is the entrance width and h is the water depth in the bay (Bruun 1978). As the jet spreads its velocity u decreases and a delta is formed beyond a distance $\zeta=L_s$, where $u<u_{cr}$, the critical velocity for erosion. From flow continuity

$$u(L_s) = u_{cr} = \frac{\overline{Q}}{w(L_s)h} \tag{23}$$

The critical velocity is obtained from Eqs. 8 and 9 as

$$u_{cr} = \left[\frac{8g\psi_{cr}}{f}(s-1)\right]^{1/2} d^{1/2} \tag{24}$$

where ψ_{cr} is the critical value of the Shields' parameter. We now combine Eqs. 3, 22, 23, and 24 to obtain

$$L_s = \frac{16h}{f}\ln\left(\frac{\frac{2}{T}\left(\frac{A_c}{a}\right)^{1/2}}{w_c h\left[\frac{8g\psi_{cr}}{f}(s-1)\right]^{1/2} d^{1/2}}\right) \tag{25}$$

By conveniently taking w_f to be the jet width at distance L_s, this width can be obtained from Eq. 22. We will consider Sikes Cut with characteristic parameters: h=3.4 m, A_c=360 m^2 (at ζ=0, the jet origin), w_c=65 m (at ζ=0), T=86,400 s, a=6.25×10^{-5}, m=1, d=3×10^{-3} m, f=0.025, ψ_{cr}=0.06, and s=2.65. This yields L_s=170 m, and from Eq. 22 (with ζ=170 m), w_f=71 m. Figure 7 appears to corroborate this value of L_s as the approximate distance beyond which the flood delta occurs. The delta has fanned out in an "explosive" mode, consistent with a rapidly widening flow jet. Such a behavior is prominent when the depth h decreases with distance, i.e., when the bay is shallower than the entrance. An extension of Eq. 22, which

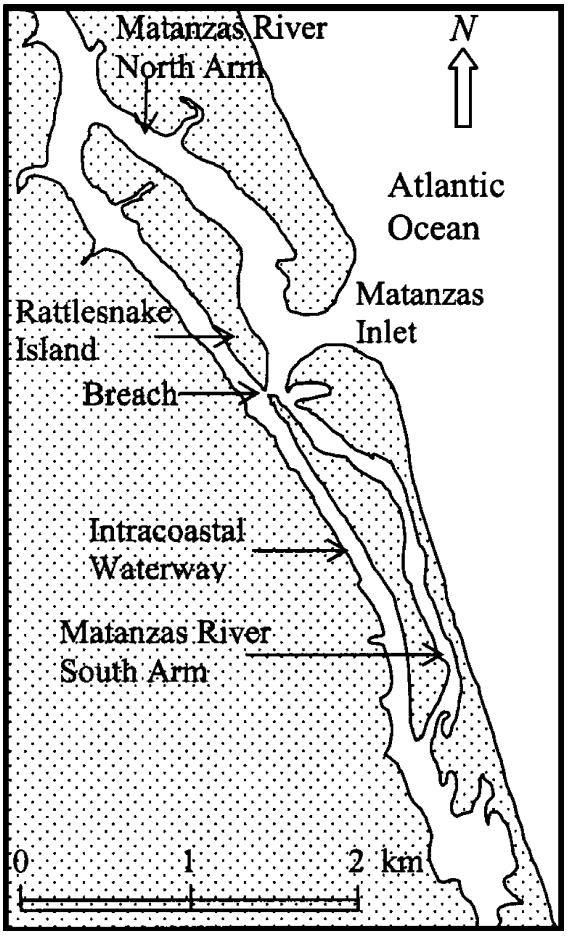

Fig. 9 Matanzas Inlet on the Atlantic Coast of Florida

Table 8 Effect of breach closure at Matanzas Inlet on ebb delta volume

Date	Tidal prism		Throat area		Ebb delta	
	Prism, P (m^3)	Change (%)	Area, A_c (m^2)	Change (%)	Volume, V_e (m^3)	Change (%)
Oct 1976	1.15×10^7	–	817	–	3.00×10^6	–
Apr 1977	5.16×10^6	−55	697	−15	2.00×10^6	−33
			323 (est.)	−61	1.09×10^6 (est.)	
1996	1.40×10^7	+171	910	+31	4.80×10^6	+140
			875 (est.)	+26	3.84×10^6 (est.)	+92

enables the simulation of the delta fan, is given in Bruun (1978).

The wider the entrance, the greater the width of the flood delta; so, for a mature delta, as h_f and L_f may be held constant, one would infer that $w_f \sim P^{1/3}$. Thus, from Eq. 21, we obtain $V_f \sim P^{1/3}$. In general,

$$V_f = c_f P^{n_f} \tag{26}$$

where c_f and n_f have qualitatively the same meaning as c_e and n_e, respectively. These coefficients are given in Table 7 based on 57 entrances in Tables 3 and 4. The prism correlates much more weakly with V_f (with low r^2 values in Table 7) than with V_e (higher r^2, Table 6). For all entrances combined, n_f is 0.34, i.e., nearly one third. The Atlantic Coast entrances by themselves show no correlation, possibly due to significant dredging at several entrances. A case in point is St. Marys Entrance, where the flood delta actually decreased from 5.5 to 1.6×10^6 m^3 when the channel was deepened between 1984 and 1992. On the Gulf Coast, the correlation improves (r^2 increases from 0.38 to 0.47) if Clam Pass, which has a small delta that may not be mature, is excluded from the best-fit analysis (Fig. 8).

An application

Matanzas Inlet on the Atlantic Coast offers a case where we may test the area–prism and ebb delta volume vs prism relationships. In 1964, Hurricane Dora broke through the narrow Rattlesnake Island separating Matanzas River from the Intracoastal Waterway (Fig. 9). By 1976, the breach was transporting 71% of the tidal prism, and the resulting cross-current was adversely affecting navigation in the waterway. In December 1976, the breach was closed by placement of rock and sand. The outcome is summarized in Table 8. Comparing the April 1977 post-closure prism, throat area, and ebb delta volume with the corresponding pre-closure values of October 1976, we observe that, due to a partial loss of the effective bay area, the prism decreased by 55%. This decrease concurrently caused the throat area to contract by 15%. One million cubic meters of sand representing about 33% of the ebb delta moved into the entrance channel and nearly blocked it (Mehta and Sheppard 1979). A portion of sand moved from the channel into the northern arm of the Matanzas River, blocking vessel access between the Intracoastal Waterway and the entrance.

Based on the line in Fig. 2, the estimated equilibrium throat area in April 1977 would be 323 m^2, as opposed to 697 m^2 achieved. From Table 6 (Atlantic Coast entrances), the equilibrium ebb delta volume is estimated to be 1.09 vs 2.00×10^6 m^3 realized. These observations imply that the 4-month period, between breach closure in December 1976 and the next bathymetric survey in April 1977, was insufficient for the entrance morphology to adjust to the decreased tidal prism.

To recover the prism, a relief channel was dredged through the northern arm of the river. This operation was successful and resulted in a 171% increase of the prism by 1996. The throat area increased by 31% (to 910 m^2), which compares favorably with a 26% increase in the estimated equilibrium area (875 m^2). The ebb delta concurrently increased by 140% to 4.80×10^6 m^3. The corresponding estimated value is 3.84×10^6 m^3, amounting to a 92% increase. This is lower than 140% but can be taken to be of the same order of magnitude.

Concluding comments

The relationship between tide-mean water discharge and flood- or ebb-mean sediment load can be construed as an indicator of the dependence of ebb and flood delta volumes on the tidal prism. The morphodynamic relationship between ebb delta volume and tidal prism, originally reported by Walton and Adams (1976), results from scaling arguments for delta geometry. For the coast of Florida as a whole, the volume varies linearly with the prism and, on that basis, is one fifth of the prism. The main source of sand in the deltas is the littoral zone as opposed to the river.

The flood delta volumes for the coast of Florida indicate that the volume at mature deltas varies with prism to a power close to one third. Scaling arguments similar to those for the ebb delta show that this dependence is consistent with the morphodynamics of flood delta development. The Atlantic Coast delta volumes by themselves do not show any correlation with the prism presumably because, at many entrances, the depths have been altered by dredging.

The effect of the closure of a storm-induced breach near Matanzas Inlet illustrates the applicability of the area–prism and ebb delta volume vs prism relationships. Four

months after breach closure and concomitant changes in the entrance morphology, the throat area reduction was over-predicted, as was the reduction in ebb delta volume. However, after several years, as the entrance reverted to a new state of equilibrium, the predicted changes in the throat area and the ebb delta volume were of the same order of magnitude as those experienced. We, therefore, conclude that the morphodynamic relationships are useful for the prediction of changes in the throat area and the ebb delta volume when morphologic changes occur over time scales consistent with the reestablishment of equilibrium.

References

Blench T (1961) Hydraulics of canals and rivers of mobile boundary. Butterworth's civil engineering reference book, 2nd edn. Butterworth, London

Bruun P (1978) Stability of tidal inlets: theory and engineering. Elsevier, Amsterdam

Carr de Betts EE, Mehta AJ (2001) An assessment of inlet flood deltas in Florida. In: Hanson H, Larson M (eds) Proceedings of the 4th conference on coastal dynamics. American Society of Civil Engineers, Reston, VA, pp 252–262

Christensen BA, Chiu TY (1973) Water and air transport of cohesionless materials. Proceedings of the 15th Congress of IAHR, vol 1. Istanbul, Turkey, pp A32-1–A32-8

Dean RG, Walton TL Jr (1975) Sediment transport processes in the vicinity of inlets with special reference to sand trapping. In: Cronin LE (ed) Estuarine research, vol II. Academic, New York, pp 129–149

Devine PT, Mehta AJ (1999) Modulation of microtidal inlet ebb deltas by severe sea. In: Kraus NC, McDougal WG (eds) Proceedings of coastal sediments 1999. American Society of Civil Engineers, Reston, VA, pp 1387–1401

De Vriend HJ, Dronkers J, Stive MJF, van Dongeren A, Wang JH (2002) Coastal inlets and tidal basins. Report CT5303. Division of Hydraulic and Offshore Engineering, Technical University of Delft, Delft, The Netherlands

Dombrowski MR, Mehta AJ (1996) Ebb tidal delta evolution of coastal inlets. Proceedings of the 25th coastal engineering conference. American Society of Civil Engineers, New York, pp 3270–3283

Gibeaut JC, Davis RA Jr (1993) Statistical geomorphologic classification of ebb-tidal deltas along the west-central Florida coast. J Coast Res 18:165–184

Graf WH (1971) Hydraulics of sediment transport. McGraw-Hill, New York

Jarrett JT (1976) Tidal prism–inlet area relationships. GITI report no. 3. Coastal Engineering Research Center, US Army Corps of Engineers, Fort Belvoir, VA

Jones CP, Mehta AJ (1980) Inlet sand bypassing systems in Florida. Shore Beach 48(1):25–34

Kraus NC (1998) Inlet cross-section area calculated by process-based model. Proceedings of coastal engineering 1998. American Society of Civil Engineers, Reston, VA, pp 3265–3278

LeConte LJ (1905) Discussion on the paper, "Notes on the improvement of river and harbor outlets in the United States" by D. A. Watt, paper no. 1009. Trans Am Soc Civ Eng 55 (December):306–308

Mason C (1973) Regime equations and tidal inlets. J Waterway Port Coast Ocean Eng 99(3):393–397

Mehta AJ, Sheppard DM (1979) Performance study at Matanzas closure. Report no. UFL/COEL-79/007. Coastal and Oceanographic Engineering Department, University of Florida, Gainesville

O'Brien MP (1969) Equilibrium flow areas of inlets on sandy coasts. J Waterway Port Coast Ocean Eng 95(1):43–52

Powell MA (2003) Ebb shoal and flood shoal volumes on the coasts of Florida: St. Mary entrance to Pensacola Pass. Report no. UFL/COEL/MPR-2003/002. Coastal and Oceanographic Engineering Program, Department of Civil and Coastal Engineering, University of Florida, Gainesville

Vincent CL, Corson WD (1981) Geometry of tidal inlets: empirical equations. J Waterw Port Coast Ocean Div 107(1):1–9

Walton TL, Adams WD (1976) Capacity of inlet outer bars to store sand. Proceedings of the 15th international conference on coastal engineering. American Society of Civil Engineers, New York, pp 1919–1937